miR-9 alleviated the inflammatory response and apoptosis in caerulein-induced acute pancreatitis by regulating FGF10 and the NF-κB signaling pathway

YANG SHEN, CHENGJUN XUE, GUOLI YOU and CUI LIU

Department of Gastroenterology, Jiangsu Hospital, Nantong University, Nantong, Jiangsu 224700, P.R. China

Received July 23, 2019; Accepted January 6, 2021

DOI: 10.3892/etm.2021.10227

Abstract. MicroRNAs (miRs) have been implicated in the development of acute pancreatitis (AP). However, the role and potential mechanism of miR-9 in AP progression remains unclear. Caerulein-treated AR42J cells were used as a cellular model of AP. Results revealed caerulein triggered an inflammatory response by promoting the secretion of inflammatory cytokines [tumor necrosis factor-α, interleukin (IL) 1β and IL-6], as evidenced by ELISA. Furthermore, caerulein-induced apoptosis was reported by flow cytometry and western blot assays. Additionally, miR-9 expression was downregulated by caerulein treatment, as demonstrated by reverse transcription quantitative PCR. However, miR-9 overexpression reduced the inflammatory response and apoptosis in caerulein-treated AR42J cells. miR-9 knockdown resulted in opposite effects. Furthermore, fibroblast growth factor (FGF) 10 was validated to be targeted via miR-9 by luciferase, RNA immunoprecipitation and RNA pull-down assays. Results demonstrated increased FGF10 expression in caerulein-treated AR42J cells and that FGF10 overexpression exacerbated the caerulein-induced inflammatory response and apoptosis, while its knockdown had the opposite effect. Additionally, FGF10 reversed the effect of miR-9 on caerulein-induced injury in AR42J cells. Results demonstrated that miR-9 inhibited the expression of the nuclear factor κB (NF-κB) pathway-related proteins by downregulating FGF10. As a result, miR-9 decreased inflammatory response and apoptosis in caerulein-treated AR42J cells by targeting FGF10 and blocking NF-κB signaling, suggesting that miR-9 may serve as a novel target for AP treatment.

Correspondence to: Dr Yang Shen, Department of Gastroenterology, Jiangsu Hospital, Nantong University, 163 East Webhui Road, Nantong, Jiangsu 224700, P.R. China
E-mail: i05800597menron@163.com

Key words: acute pancreatitis, microRNA 9, fibroblast growth factor 10, inflammatory response, apoptosis

Introduction

Acute pancreatitis (AP) is a common clinical condition characterized by pancreatic edema and inflammation (1) that leads to poor outcomes, such as organ failure and necrosis (2). Pancreatic inflammation and acinar cell death (including apoptosis) are the major pathophysiological features of AP (3-5). Caerulein, a cholecystokinin analog, causes intra-acinar activation of trypsinogen in the pancreas, which can lead to AP-like symptoms (6). The downregulation of Bcl-2 and the upregulation of Bax and activated caspase 3/9 are associated with caerulein-induced apoptosis of acinar cells in AP (7-9). Hence, elucidating the mechanism of caerulein-induced pancreatic acinar cell injury is crucial to identify therapeutic targets for AP.

MicroRNAs (miRs) are single-stranded non-coding RNAs that serve essential roles in inflammatory diseases, including AP (10). For example, Fu *et al* (11) reported that, by targeting tumor necrosis factor (TNF) receptor 1A, miR-29 was upregulated and subsequently promoted AR42J cell apoptosis, which were used as the cellular model of AP. Furthermore, Zhang *et al* (12) demonstrated that miR-551b-5p promoted the inflammatory response and AP progression. miR-9 has been reported to act as an oncogene or tumor inhibitor in various types of tumor, such as synovial sarcoma and pancreatic cancer (13,14). Bone marrow-derived mesenchymal stem cells have been demonstrated to upregulate miR-9 to inhibit the inflammatory response and necroptosis in AP rats (15). Furthermore, a previous study hypothesized that miR-9 may be associated with the nuclear factor κB (NF-κB) pathway and p50 (16). These results suggested that miR-9 may exert a therapeutic effect in AP. However, its mechanism of action remains unclear and further research into the role of miR-9 is required to elucidate the pathway of AP pathogenesis.

Growth factors, including vascular endothelial growth factor, transforming growth factor and fibroblast growth factor (FGF), have been implicated in AP pathogenesis and pancreatic carcinoma (17). FGF10 is a member of the FGF family, which is associated with the development of the pancreas (18). Activation of NF-κB signaling is a critical event in AP development (19) and miR-9 and FGF10 have been reported to be essential mediators of this pathway in human disease (20-23).

The aim of the present study was to explore the function of miR-9 on the inflammatory response and apoptosis in caerulein-treated AR42J cells, and to analyze the interaction between miR-9 and the FGF10/NF-κB pathway.

Materials and methods

AP cell model and cell transfection. Rat pancreatic acinar AR42J cells (American Type Culture Collection) were cultured in RPMI-1640 medium (Gibco; Thermo Fisher Scientific, Inc.) supplemented with 10% FBS (Gibco; Thermo Fisher Scientific, Inc.) at 37˚C and 5% CO_2. AR42J cells were then incubated with 10 nM caerulein (Sigma-Aldrich, Merck KGaA) at 37˚C for 0, 2, 4, 6 or 8 h to establish an *in vitro* model of AP. An untreated group was regarded as the control.

miR-9 mimic (miR-9; 5'-UCUUUGGUUAUCUAGCUG UAUGA-3'), mimic negative control (miR-NC; 5'-CGAUCG CAUCAGCAUCGAUUGC-3'), miR-9 inhibitor (anti-miR-9; 5'-UCAUACAGCUAGAUAACCAAAGA-3'), inhibitor negative control (anti-miR-NC; 5'-CAGUACUUUUGU GUAGUACAA-3'), small interfering RNA (siRNA) against FGF10 (si-FGF10; 5'-UGUUGUAUCCAUUUUCCUCUA-3'), siRNA negative control (si-NC; 5'-AAGACAUUGUGUGUC CGCCTT-3'), pcDNA-based FGF10 overexpression vector (pc-FGF10) and pcDNA negative control (pc-NC) were generated by Shanghai GenePharma, Co., Ltd. Vectors (1 μg) and miRNA or siRNA oligos (20 nM) were then transfected into AR42J cells using Lipofectamine® 2000 (Thermo Fisher Scientific, Inc.), according to the manufacturer's protocol. Following 24 h incubation at 37˚C, cells were harvested for caerulein treatment. A group that did not undergo transfection was regarded as the control.

ELISA. AR42J cells were seeded into 24-well plates ($4x10^4$ per well) in sextuplicate and subjected to the treatment with 10 nM caerulein at 37˚C for 0, 2, 4, 6 or 8 h. Cell culture supernatant was collected after centrifugation at 1,000 x g at room temperature for 10 min. The concentration of TNF-α, IL-1β and IL-6 inflammatory cytokines were measured using specific TNF-α (cat. no. BMS622), IL-1β (cat. no. BMS630) and IL-6 (cat. no. BMS625) rat ELISA kits (Thermo Fisher Scientific, Inc.), according to the manufacturer's protocol. The optical density was determined at a wavelength of 450 nm using an iMark microplate reader (Bio-Rad Laboratories, Inc.). The concentrations were determined from the standard curve.

Cell apoptosis. Flow cytometry was performed using an Annexin V-FITC/PI apoptosis detection kit (Beyotime Institute of Biotechnology), according to the manufacturer's protocol. Transfected or non-transfected AR42J cells ($1x10^5$ cells/well) were seeded into 6-well plates in triplicate overnight at 37˚C. Following 10 nM caerulein incubation at 37˚C for 0, 2, 4, 6 or 8 h cells were collected and incubated with 10 μl Annexin V-FITC and PI solution in the dark at room temperature for 10 min. Apoptotic cells were analyzed using a FACSCalibur flow cytometer (Becton Dickinson) with CellQuest Pro 3.0 software (Becton Dickinson). The apoptotic rate was displayed as the percentage of cells exhibiting positive Annexin V-FITC and positive/negative PI.

Western blotting. AR42J cells were harvested and lysed in RIPA lysis buffer (Beyotime Institute of Biotechnology) and protein samples were quantified using a BCA protein assay kit (Beyotime Institute of Biotechnology) followed by denaturation in a boiling water bath for 10 min. Total protein (20 μg/lane) was separated by 10% SDS-PAGE and transferred onto nitrocellulose membranes (EMD Millipore) with Tris-Glycine transfer buffer (Novex; Thermo Fisher Scientific, Inc.). Membranes were incubated with 5% non-fat milk at room temperature for 1 h to block non-specific binding sites, followed by incubation with primary antibodies overnight at 4˚C and secondary antibodies at room temperature for 2 h. Primary antibodies anti-Bcl-2 (cat. no. ab196495; 1:1,000; Abcam), anti-Bax (cat. no. ab53154; 1:1,000; Abcam), anti-pro-caspase 3 and anti-cleaved (cl) caspase 3 (cat. no. 14220; 1:1,000; Cell Signaling Technology, Inc.), anti-pro-caspase 9 and anti-cl caspase 9 (cat. no. 9508; 1:1,000; Cell Signaling Technology, Inc.), anti-FGF10 (cat. no. ab227102; 1:3,000; Abcam) anti-NF-kappa-B inhibitor alpha (IKBα; cat. no. ab7217; 1:2,000; Abcam), anti-NFKB1 (subunit p50; cat. no. ab32360; 1:5,000; Abcam), anti-p-p65 (cat. no. ab86299; 1:2,000; Abcam), anti-total-p65 (cat. no. ab16502; 1:1,000; Abcam), anti-GAPDH (cat. no. ab181603; 1:10,000; Abcam) and horseradish peroxidase-conjugated IgG secondary antibodies (cat. nos. ab205718 and ab205719; 1:10,000; Abcam). Protein signals were developed and visualized utilizing enhanced chemiluminescence Western Blotting Substrate reagent (Pierce; Thermo Fisher Scientific, Inc.). Relative protein level was normalized to GAPDH following densitometry analysis using Image Lab 3.0 software (Bio-Rad Laboratories, Inc.). All experiments were performed in triplicate.

Reverse transcription quantitative PCR (RT-qPCR). Total RNA was extracted from AR42J cells following incubation with TRIzol® reagent (Thermo Fisher Scientific, Inc.), according to the manufacturer's protocol. RNA (1 μg) was reverse transcribed (denaturation at 65˚C for 15 min, followed by reaction at 25˚C for 10 min and 42˚C for 60 min, and denaturation at 99˚C for 5 min) using a first-strand cDNA kit (Sigma-Aldrich, Merck KGaA) according to the manufacturer's protocol. RT-qPCR was performed using cDNA, specific primers and SYBR™ Green (Takara Bio, Inc.) on a 7500 RT-q PCR system (Applied Biosystems; Thermo Fisher Scientific, Inc.). The thermocycling conditions were 95˚C for 5 min and 40 cycles, 95˚C for 15 sec and 60˚C for 1 min, followed by 72˚C for 5 min. The following pairs of rat RNA primers were used: FGF10 forward, 5'-AAGAACGGCAAGGTCAGC-3' and reverse, 5'-GAGGAAGTGAGCGGAGGTG-3'; GAPDH forward, 5'-GACATGCCGCCTGGAGAAAC-3' and reverse, 5'-AGCCCAGGATGCCCTTTAGT-3'; miR-9 forward, 5'-GCCCGCTCTTTGGTTATCTAG-3' and reverse, 5'-CCA GTGCAGGGTCCGAGGT-3'; and U6 forward, 5'-CTCGCT TCGGCAGCACA-3' and reverse, 5'-AACGCTTCACGAATT TGCGT-3'. FGF10 and miR-9 expressions were normalized to U6 or GAPDH, respectively and calculated according to the $2^{-\Delta\Delta Cq}$ method (24). All experiments were performed in triplicate.

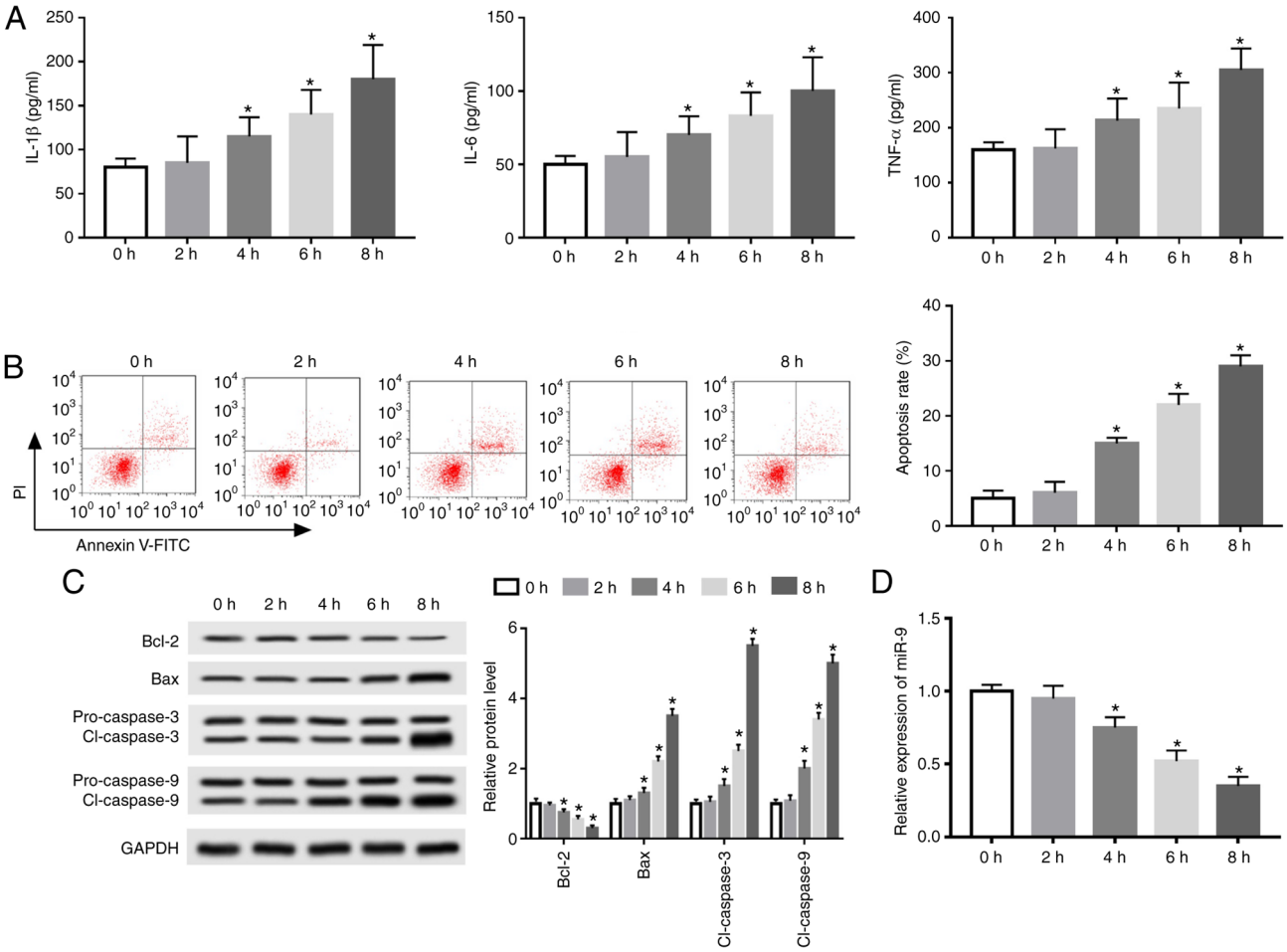

Figure 1. miR-9 expression is decreased in a caerulein-induced cellular model of acute pancreatitis. (A) Inflammatory cytokine expression, including IL-1β, IL-6 and TNF-α, was measured by ELISA. (B) Apoptosis rate was measured via flow cytometry. (C) Apoptotic-associated protein expression was detected via western blotting. (D) miR-9 expression was measured by reverse transcription-quantitative PCR. Data are presented as mean ± standard deviation. *P<0.05 vs. the control (0 h) group. miR, microRNA; IL, interleukin; TNF, tumor necrosis factor; Bcl-2, B-cell lymphoma 2; Bax, Bcl-2 associated X; cl-caspase, cleaved caspase.

Bioinformatics analysis and luciferase reporter assay. Bioinformatics analysis using TargetScan 7.2 (targetscan.org/vert_72) indicated there were binding sites between miR-9 and FGF10. FGF10 3' untranslated (UTR) sequences containing miR-9 binding sites (ACCAAAG) were amplified and cloned into pmirGLO vectors (Promega Corporation) to generate wild type luciferase (wt-FGF10) and mutant (mut-FGF10) vectors by mutating the seed sites to UGGUUUC using a Fast Site-Directed Mutagenesis kit (Tiangen Biotech Co., Ltd.) according to the manufacturer's protocol.

Luciferase reporter assay was performed in AR42J cells after co-transfection with wt-FGF10 or mut-FGF10 and miR-NC, miR-9 mimic, anti-miR-NC or anti-miR-9 using Lipofectamine® 2000 (Thermo Fisher Scientific, Inc.). Cells were harvested 24 h post-transfection and luciferase activity was measured using a Dual-Glo luciferase assay system (Promega Corporation) by normalizing to Renilla luciferase. All experiments were performed in triplicate.

RNA immunoprecipitation (RIP). A magna RNA immunoprecipitation kit (EMD Millipore) was used on AR42J cells for RIP according to the manufacturer's protocol. Cells were lysed with RIP lysis buffer containing proteinase and RNase inhibitors (provided in the kit) and incubated with magnetic beads pre-coated with anti-argonaute-2 (Ago2) antibodies (cat. no. ab32381; Abcam) for 6 h at 4˚C. Immunoglobulin G (IgG; cat. no. AP112; Sigma-Aldrich; Merck KGaA) and cell lysates were used as controls. The beads were then washed with RIP washing buffer and the immunoprecipitate was digested with proteinase K (provided in the kit). FGF10 and miR-9 RNA levels were detected via RT-qPCR as describe above. All experiments were performed in triplicate.

RNA pull-down assay. An RNA pull-down assay was performed using an RNA-Protein pull-down kit (Thermo Fisher Scientific, Inc.) according to the manufacturer's protocol. Biotinylated FGF10 (bio-FGF10-wt), mutant FGF10 (bio-FGF10-mut) and negative control (bio-NC) probes were designed by Guangzhou RiboBio Co., Ltd. and conjugated with streptavidin magnetic beads (Thermo Fisher Scientific, Inc.). AR42J cells were lysed using RIP lysis buffer, and incubated with probe-coated beads for 2 h at 4˚C. Beads were then washed with washing buffer (provided in the kit), and the biotin-coupled RNA complex was pulled down using elution buffer by vortexing. Enriched miR-9 levels were analyzed via RT-qPCR as described above. All experiments were performed in triplicate.

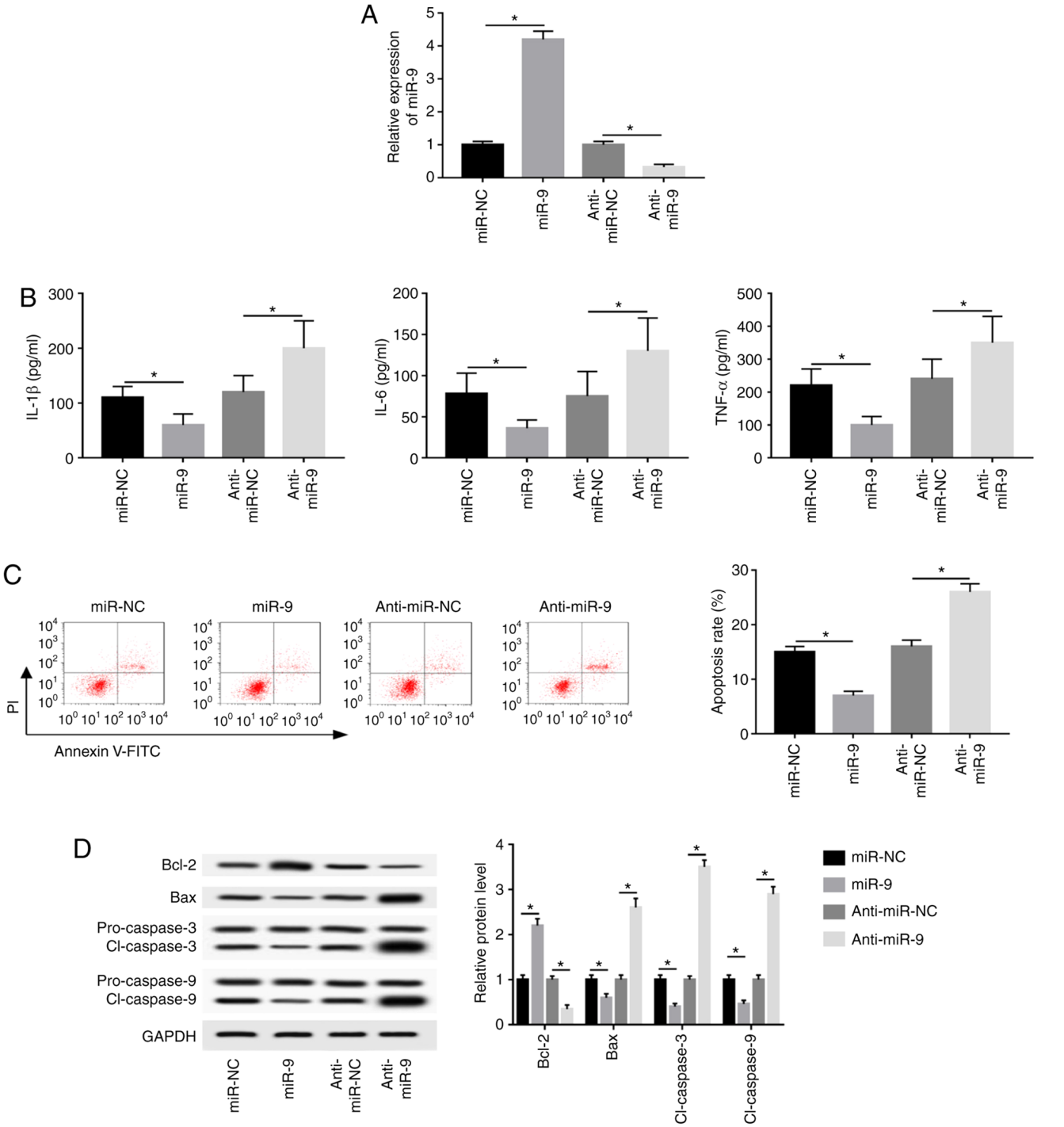

Figure 2. miR-9 inhibits caerulein-induced inflammatory response and apoptosis in AR42J cells. AR42J cells were transfected with miR-NC, miR-9, anti-miR-NC or anti-miR-9 prior to caerulein treatment. (A) miR-9 expression, (B) inflammatory cytokine levels (C) apoptotic rate and (D) apoptotic-related protein levels were detected in the treated cells by reverse transcription quantitative PCR, ELISA, flow cytometry and western blotting, respectively. Data are presented as the mean ± SD. *P<0.05, as indicated. miR, microRNA; miR-NC, mimic negative control; miR-9, mir-9 mimic; anti-miR-NC, inhibitor negative control; anti-miR-9, miR-9 inhibitor; IL, interleukin; TNF, tumor necrosis factor; PI, propidium iodide; FITC, fluorescein isothiocyanate; Bcl-2, B-cell lymphoma 2; Bax, Bcl-2 associated X; cl-caspase, cleaved caspase.

Statistical analysis. Statistical analysis was performed using GraphPad Prism software (version 7; GraphPad Software, Inc.). Data are presented as the mean ± standard deviation. Student's t-test or one-way ANOVA followed by Tukey's post hoc test was performed to compare differences between groups, as applicable. P<0.05 was considered to indicate a statistically significant difference.

Results

miR-9 expression is reduced in caerulein-treated AR42J cells. An AP model was established using caerulein-treated AR42J cells to investigate the potential role of miR-9 in AP progression. IL-1β, IL-6 and TNF-α levels were elevated in a time-dependent manner following treatment for 0-8 h

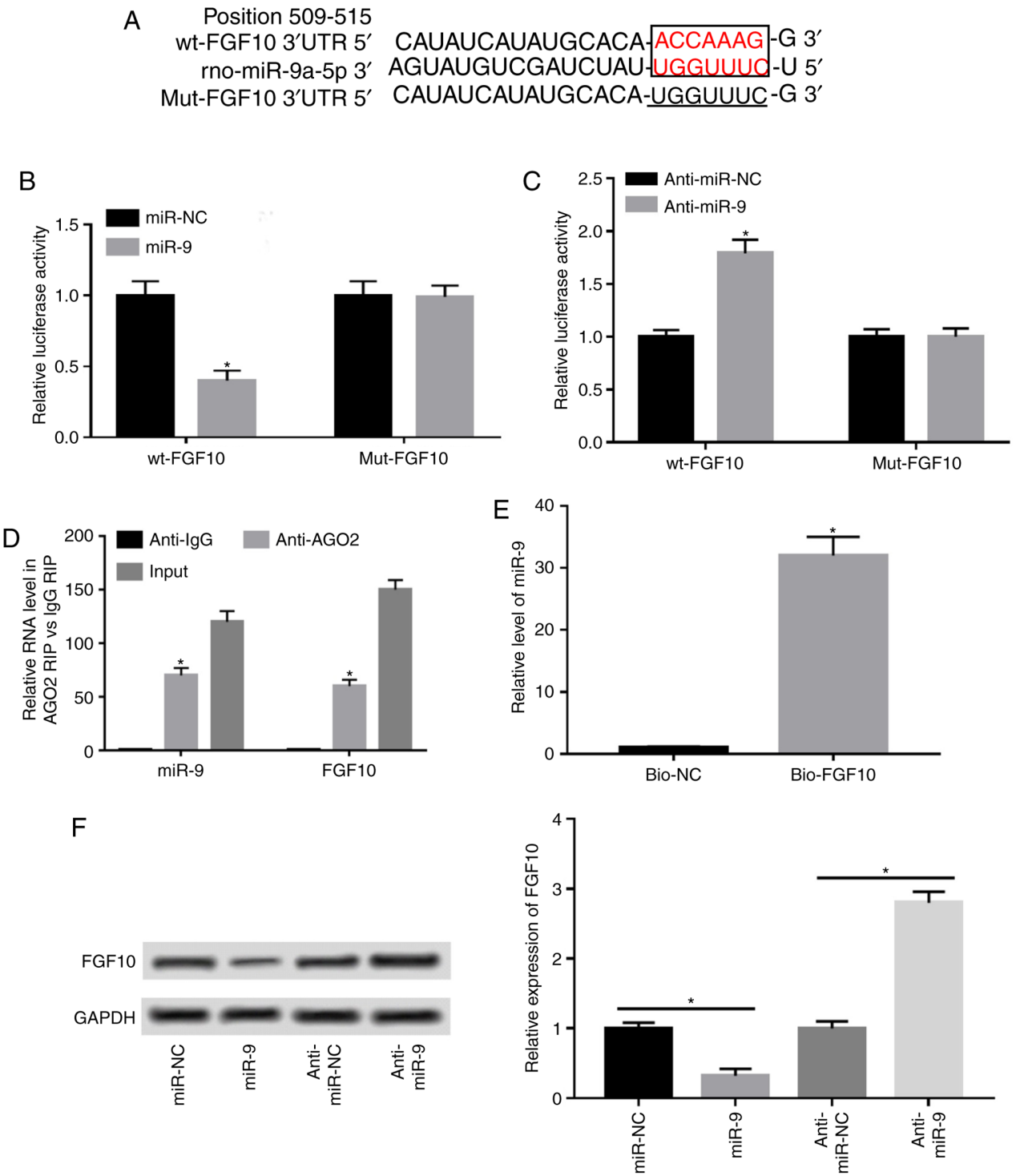

Figure 3. FGF10 is a target of miR-9 in caurulein-treated AR42J cells. (A) Predicted binding sites of miR-9 and FGF10 generated by TargetScan. Binding sites are presented in red and mutant sites are underlined. Luciferase reporter assay was performed in cells co-transfected with (B) wt-FGF10 or mut-FGF10 and miR-NC, miR-9, (C) anti-miR-NC or anti-miR-9. (D) Ago2 RIP assay was performed and miR-9 and FGF10 levels were measured via RT-qPCR. (E) RNA pull-down assay was performed in AR42J cells and miR-9 expression was detected via RT-qPCR. (F) FGF10 expression was detected in cells transfected with miR-NC, miR-9 mimic, anti-miR-NC or anti-miR-9 via western blotting. Data are presented as the mean ± standard deviation. *P<0.05 as indicated. FGF10, fibroblast growth factor 10; wt, wild type; mut, mutant; miR-NC, mimic negative control; miR-9, miR-9 mimic; anti-miR-NC, inhibitor negative control; anti-miR-9, miR-9 inhibitor; Ago2, protein argonaute-2; RIP, RNA immunoprecipitation; RT-qPCR, reverse transcription quantitative PCR; IgG, immunoglobulin G; bio-NC, negative control; bio-FGF10-wt, biotinylated FGF10; bio-FGF10-mut, biotinylated mutant FGF10; input, cell lysates as the positive control.

(Fig. 1A). Furthermore, flow cytometry data revealed that caerulein treatment induced apoptosis in a time-dependent manner (Fig. 1B). Western blotting also demonstrated that exposure to caerulein decreased Bcl-2 expression and increased Bax and cl-caspase 3 and 9 expression time-dependently (Fig. 1C). The results indicated that caerulein induced an inflammatory response and apoptosis in caerulein-treated AR42J cells.

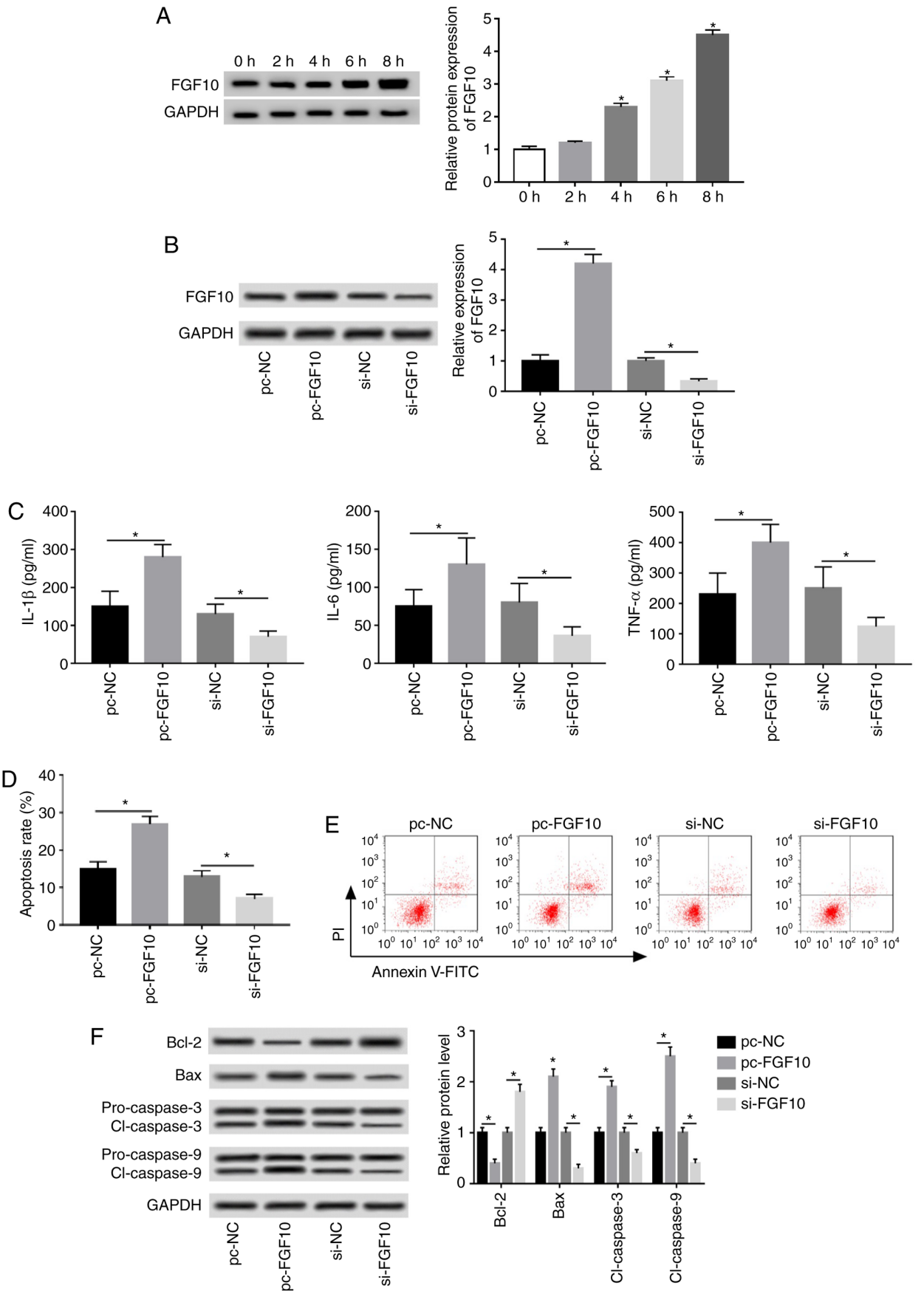

Figure 4. FGF10 promotes caerulein-induced inflammatory response and apoptosis in AR42J cells. (A) FGF10 expression was measured following treatment at different time points via western blotting. Cells were transfected with pc-NC, pc-FGF10, si-NC or si-FGF10 and (B) FGF10 expression, (C) inflammatory cytokine levels, (D) apoptotic rate, (E) cell apoptosis and (F) apoptotic-associated protein expression were detected via western blotting, ELISA and flow cytometry. Data are presented as the mean ± standard deviation. *P<0.05 as indicated. FGF10, fibroblast growth factor 10; pc-NC, pcDNA empty vector; pc-FGF10, pcDNA-based FGF10 overexpression vector; si-NC, siRNA negative control; si-FGF10, small interfering RNA against FGF10; IL, interleukin; TNF, tumor necrosis factor; Bcl-2, B-cell lymphoma 2; Bax, Bcl-2 associated X; cl-caspase, cleaved caspase.

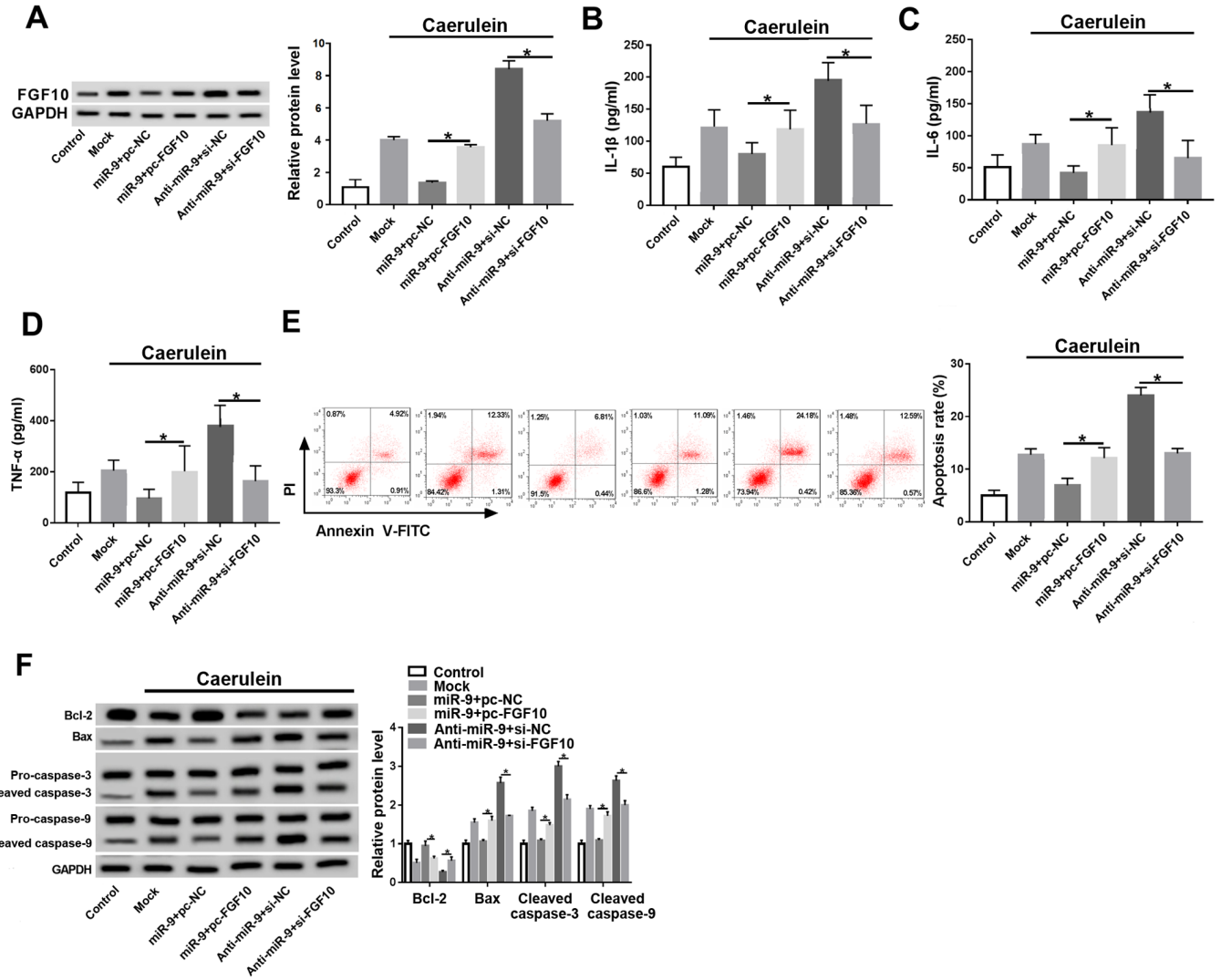

Figure 5. FGF10 reverses the miR-9-mediated inflammatory response and apoptosis in caerulein-treated AR42J cells. (A) FGF10 expression, inflammatory cytokine (B) IL-1β, (C) IL-6 and (D) TNF-α levels, (E) apoptotic rate and (F) apoptotic-associated protein expressions were detected in cells transfected with miR-9 and pc-NC or pc-FGF10, anti-miR-9 and si-NC or si-FGF10 by ELISA, flow cytometry and western blotting. Data are presented as the mean ± standard deviation. *P<0.05 as indicated. FGF10, fibroblast growth factor 10; miR, microRNA; miR-9, miR-9 mimic; pc-NC, pcDNA empty vector; pc-FGF10, pcDNA-based FGF10 overexpression vector; anti-miR, miR-9 inhibitor; si-NC, siRNA negative control; si-FGF10, siRNA against FGF10; Mock, non-transfected group; IL, interleukin; TNF, tumor necrosis factor; Bcl-2, B-cell lymphoma 2; Bax, Bcl-2 associated X; cl-caspase, cleaved caspase.

Additionally, miR-9 expression was measured in caerulein-induced AR42J cells. The results revealed that miR-9 expression was significantly decreased in a time-dependent manner (Fig. 1D). The optimum time of caerulein exposure was determined to be 8 h.

miR-9 decreases the inflammatory response and apoptosis in caerulein-treated AR42J cells. AR42J cells were transfected with miR-NC, miR-9 mimic, anti-miR-NC or anti-miR-9 and treated for 8 h to investigate the effect of miR-9 on caerulein-induced injury. miR-9 expression was upregulated 4.2-fold in the miR-9 mimic group, while anti-miR-9-transfected cells demonstrated a 68% reduction in miR-9 expression compared with corresponding controls (Fig. 2A). Furthermore, miR-9 overexpression significantly inhibited IL-1β, IL-6 and TNF-α expression, while miR-9 knockdown exerted the opposite effect (Fig. 2B). Additionally, overexpression of miR-9 significantly decreased caerulein-induced apoptosis, whereas miR-9 knockdown significantly promoted cell apoptosis (Fig. 2C). The results also demonstrated that miR-9 overexpression upregulated Bcl-2 and downregulated Bax and cl-caspases 3 and 9, while miR-9 knockdown exerted the opposite effect (Fig. 2D).

FGF10 is a target of miR9. A potential miR-9 target was investigated via bioinformatics analysis using TargetScan to elucidate the mechanism by which miR-9 regulates AP progression. Predicted binding sites between miR-9 and FGF10 at position 509-515 of the 3'UTR were exhibited and luciferase reporter vectors containing wt or mut miR-9 seeding sites were generated (Fig. 3A). The results demonstrated that miR-9 overexpression resulted in a 55% reduction in luciferase activity (Fig. 3B). Additionally, miR-9 knockdown significantly increased luciferase activity in the wt-FGF10 group, but remained unaffected in the mut-FGF10 group (Fig. 3C). Furthermore, miR-9 and FGF10 were enriched in the same

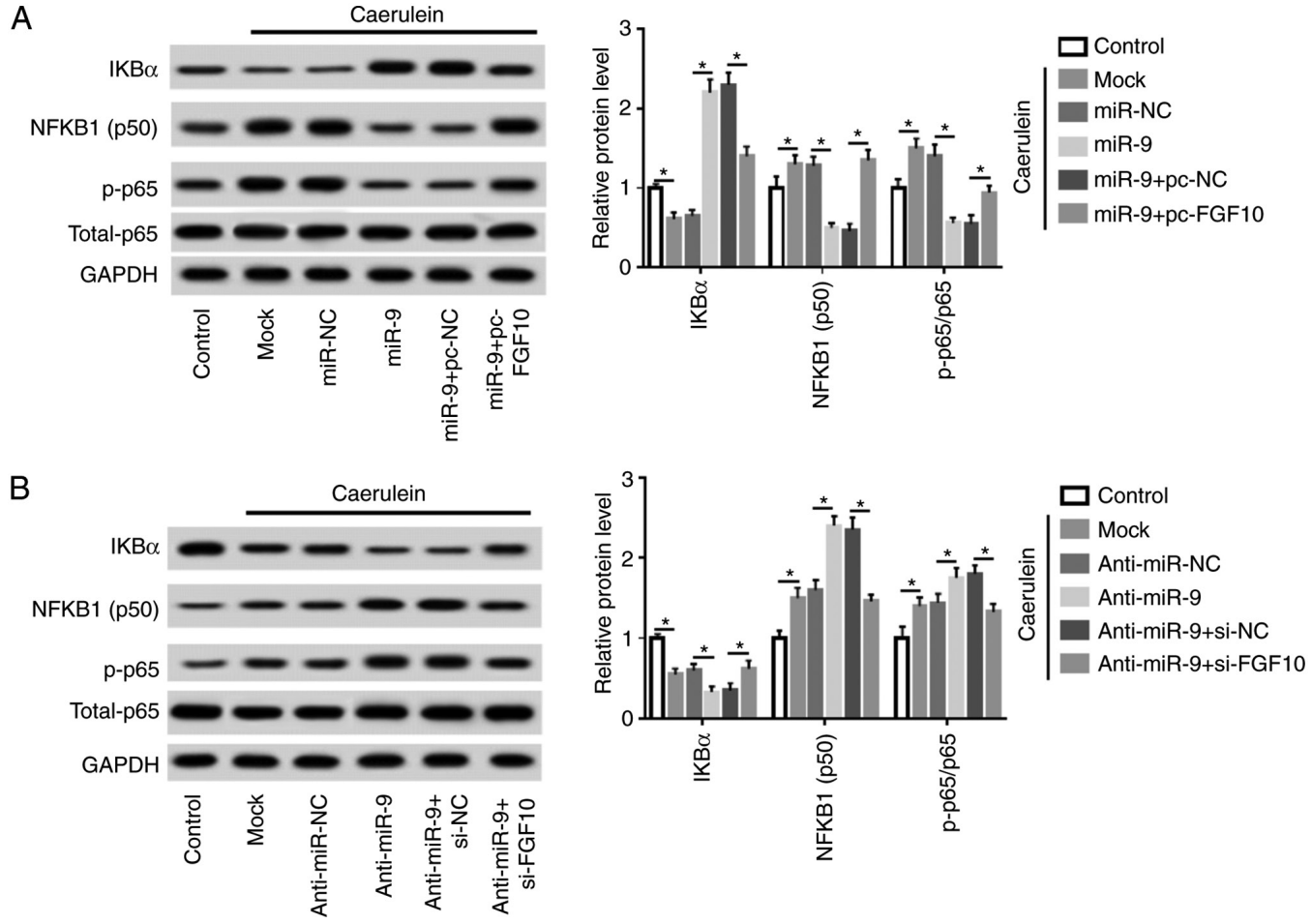

Figure 6. miR-9 inhibits the NF-κB pathway through FGF10 in caerulein-treated AR42J cells. (A) IKBα, NFKB1 (p50) and p-p65 expression was measured in AR42J cells transfected with miR-NC, miR-9 mimic, miR-9 mimic and pc-NC or pc-FGF10 after treatment of caerulein by western blotting. (B) IKBα, NF-κB subunit 1 (subunit p50) and phosphorylated p65 expression was measured in AR42J cells transfected with anti-miR-NC, anti-miR-9, anti-miR-9 + si-NC or si-FGF10 following caerulein treatment by western blotting. Data are presented as the mean ± standard deviation. *P<0.05 as indicated. IKBα, NF-kappa-B inhibitor alpha; NF-κB, nuclear factor kappa-light-chain-enhancer of activated B cells; FGF10, fibroblast growth factor 10; p-p65, p-p65; total-p65, p65 in nucleus; anti-miR-NC, inhibitor negative control; pc-NC, pcDNA empty vector; pc-FGF10; pcDNA-based FGF10 overexpression vector; mock, non-transfected group.

complex by protein Ago2 RIP compared with the IgG RIP group (Fig. 3D). RNA pull-down assay demonstrated that biotinylated FGF10 induced higher miR-9 expression compared with the negative control group, and that the binding was abolished in the bio-FGF10-mut group by mutating its binding sites (Fig. 3E). Additionally, the effect of miR-9 on FGF10 expression was analyzed by overexpressing or knocking down miR-9. The results of western blotting demonstrated that FGF10 expression was decreased by 70% when miR-9 was overexpressed and enhanced 2.8-fold by miR-9 knockdown (Fig. 3F).

FGF10 promotes inflammatory response and apoptosis in caerulein-treated AR42J cells. FGF10 expression was progressively upregulated following treatment in a time-dependent manner (Fig. 4A). Cells were transfected with pc-NC, pc-FGF10, si-NC or si-FGF10 to investigate the role of FGF10 in caerulein-induced injury. FGF10 expression was upregulated 4.2-fold by pc-FGF10 and reduced by 67% following si-FGF10 treatment, as demonstrated via western blotting (Fig. 4B). IL-1β, IL-6 and TNF-α expression was significantly increased by FGF10 overexpression and inhibited by FGF10 interference (Fig. 4C). Additionally, flow cytometry and western blotting data revealed that FGF10 overexpression significantly increased caerulein-induced apoptosis, increased apoptotic-associated protein expression (Bax, cl-caspases 3 and 9) and reduced antiapoptotic protein levels (Bcl-2). FGF10 knockdown demonstrated opposite results (Fig. 4D-F).

miR-9 regulates the inflammatory response and apoptosis by targeting FGF10 in caerulein-treated AR42J cells. Cells were co-transfected with miR-9 mimic and pc-NC or pc-FGF10, anti-miR-9 and si-NC, or si-FGF10 prior to caerulein treatment to investigate whether FGF10 was involved in miR-9-mediated AP progression *in vitro*. FGF10 expression was rescued by pc-FGF10 and decreased by si-FGF10 in the presence of the miR-9 mimic or anti-miR-9 (Fig. 5A). FGF10 restoration caused the miR-9-induced downregulation of inflammatory cytokines to be reversed, and silence of FGF10 attenuated knockdown of miR-9-induced the secretion of IL-1β, IL-6 and TNF-α (Fig. 5B-D). Furthermore, FGF10 alleviated

miR-9-mediated apoptosis inhibition and FGF10 interference counteracted the effect of miR-9 knockdown on cell apoptosis (Fig. 5E and F).

miR-9 repressed the NF-κB pathway by targeting FGF10 in caerulein-treated AR42J cells. Cells were transfected with miR-NC, miR-9 mimic, miR-9 mimic and pc-NC or pc-FGF10, anti-miR-NC, anti-miR-9, anti-miR-9 and si-NC or si-FGF10 prior to caerulein treatment. Levels of proteins involved in the NF-κB pathway were subsequently measured. Caerulein treatment led to reduction of IKBα and an increase in NFKB1 (subunit p50) and phosphorylated p65, indicating that caerulein induced NF-κB pathway activation. Additionally, miR-9 overexpression suppressed the activation of the NF-κB pathway, which was mitigated by FGF10 restoration (Fig. 6A). Furthermore, miR-9 knockdown aggravated caerulein-induced pathway activation and this effect was abolished by FGF10 silencing (Fig. 6B). Collectively, miR-9 mitigated the inflammatory response and cell apoptosis in caerulein-induced AP cells, possibly by targeting FGF10 and regulating the NF-κB pathway.

Discussion

Caerulein-treated AR42J cells were used in a model of AP *in vitro* as previously described (25-27). In the current study, AR42J cells were incubated with 10 nM caerulein for 0, 2, 4, 6 or 8 h. The results demonstrated that caerulein triggered the inflammatory response and apoptosis. The present study also investigated the role of miR-9 in caerulein-induced injury and demonstrated an association between miR-9 and FGF10 *in vitro*.

In the present study, miR-9 levels were decreased in caerulein-treated AR42J cells, suggesting that miR-9 may serve a protective role in AP development. These results are consistent with those of previous studies (16,28). However, Lu *et al* (29) reported that miR-9 was highly expressed in the serum of patients with AP and that this expression could be used as a critical diagnostic and prognostic marker of AP. The current study hypothesized that this result may have been caused by the different microenvironment observed in serum and cells.

Inflammatory response and acinar cell apoptosis are the main features of AP (26,30). A recent study reported that miR-9 inhibited apoptosis and the inflammatory response in human umbilical vascular endothelial cells (31). The current study revealed that miR-9 suppressed caerulein-induced inflammatory response by decreasing IL-1β, IL-6 and TNF-α expression and regulating Bcl-2 family proteins and caspases in AR42J cells to repress apoptosis, thereby exhibiting a potential therapeutic role of miR-9 in AP.

Functional miRs regulate mRNA expression by targeting the 3'-UTR (32). In the current study, luciferase, RIP and RNA pull-down assays revealed that miR-9 could bind to FGF10, indicating that FGF10 served as a functional target of miR-9. FGF2 has been reported to exhibit high expressions in AP and to stimulate the inflammatory response (33,34). FGF10, a high-affinity ligand of FGF2, was expressed in AP tissues, suggesting that FGF10 may contribute to AP development as it was not expressed in normal pancreas tissue (35). In the current study, gain- and loss-of-function experiments demonstrated that FGF10 promoted inflammatory cytokine secretion and apoptosis in caerulein-treated cells, indicating that FGF10 may facilitate AP progression. Furthermore, overexpression or knockdown of FGF10 attenuated the effect of miR-9 on caerulein-induced AP progression, revealing that miR-9 may attenuate AP-like injury by targeting FGF10.

Previous studies have reported that FGF10 is a vital regulator of the NF-κB-dependent inflammatory response (22,23). IKBα is a major inhibitor of NF-κB and may remove NF-κB complexes in nuclei (36). NF-κB is comprised of p50 and p65 subunits and is activated by p65, which may promote the secretion of the inflammatory cytokines IL-1β, IL-6 and TNF-α (37,38). Furthermore, the NF-κB pathway has been associated with cell apoptosis in AP (39,40). The results of the current study demonstrated that caerulein led to the activation of NF-κB signaling in AR42J cells by decreasing IKBα and increasing p50 and p65, indicating that NF-κB pathway activation was involved in AP progression. Inhibition of NF-κB signaling has been regarded as a key avenue for therapeutics of AP (41-43). Additionally, the results suggested that miR-9 inhibited the caerulein-induced activation of the NF-κB pathway, which has also been reported in previous work (16). The results of the current study revealed that this effect was associated with FGF10. Data indicated that miR-9 may target FGF10 to block the NF-κB pathway, leading to the inhibition of the inflammatory response and apoptosis in caerulein-treated cells. However, the current study only reported *in vitro* results. Further research is required to investigate the role of miR-9 *in vivo* to fully elucidate AP pathogenesis.

In conclusion, miR-9 expression was decreased in a caerulein-induced cellular model of AP. miR-9 attenuated the caerulein-induced inflammatory response and cell apoptosis, possibly by targeting FGF10 and regulating the NF-κB pathway. The current study elucidated a novel mechanism of AP pathogenesis and hypothesized a novel target for AP treatment.

Acknowledgements

Not applicable.

Funding

No funding was received.

Availability of data and materials

The datasets used and/or analyzed during the present study are available from the corresponding author on reasonable request.

Authors' contributions

YS and CL conceived and designed the present study. YS, CX and GY performed the experiments. YS and CX confirm the authenticity of all the raw data. YS and CL analyzed the data. YS and CL wrote the manuscript. All authors read and approved the final manuscript.

Ethics approval and consent to participate

Not applicable.

Patient consent for publication

Not applicable.

Competing interests

The authors declare that they have no competing interests.

References

1. Forsmark CE, Vege SS and Wilcox CM: Acute pancreatitis. N Engl J Med 375: 1972-1981, 2016.
2. Petrov MS, Shanbhag S, Chakraborty M, Phillips AR and Windsor JA: Organ failure and infection of pancreatic necrosis as determinants of mortality in patients with acute pancreatitis. Gastroenterology 139: 813-820, 2010.
3. Wang G, Qu FZ, Li L, Lv JC and Sun B: Necroptosis: A potential, promising target and switch in acute pancreatitis. Apoptosis 21: 121-129, 2016.
4. Tan JH, Cao RC, Zhou L, Zhou ZT, Chen HJ, Xu J, Chen XM, Jin YC, Lin JY, Qi ZC, *et al*: EMC6 regulates acinar apoptosis via APAF1 in acute and chronic pancreatitis. Cell Death Dis 11: 966, 2020.
5. Bansod S and Godugu C: Nimbolide ameliorates pancreatic inflammation and apoptosis by modulating NF-κB/SIRT1 and apoptosis signaling in acute pancreatitis model. Int Immunopharmacol 90: 107246, 2020.
6. Jeong YK and Kim H: A mini-review on the effect of docosahexaenoic acid (DHA) on cerulein-induced and hypertriglyceridemic acute pancreatitis. Int J Mol Sci 18: 2239, 2017.
7. Cai Y, Shen Y, Xu G, Tao R, Yuan W, Huang Z and Zhang D: TRAM1 protects AR42J cells from caerulein-induced acute pancreatitis through ER stress-apoptosis pathway. In Vitro Cell Dev Biol Anim 52: 530-536, 2016.
8. Cui L, Liu R, Li C, Yu X, Liu X, Hou F, Chi C, Yin C and Wang C: Angiotensin-(1-7) attenuates caerulein-induced pancreatic acinar cell apoptosis. Mol Med Rep 16: 3455-3460, 2017.
9. Cao S, Bian Y, Zhou X, Yuan Q, Wei S, Xue L, Yang F, Dong QQ, Wang WJ, Zheng B, *et al*: A small-molecule activator of mitochondrial aldehyde dehydrogenase 2 reduces the severity of cerulein-induced acute pancreatitis. Biochem Biophys Res Commun 522: 518-524, 2020.
10. Xiang H, Tao X, Xia S, Qu J, Song H, Liu J and Shang D: Targeting microRNA function in acute pancreatitis. Front Physiol 8: 726, 2017.
11. Fu Q, Qin T, Chen L, Liu CJ, Zhang X, Wang YZ, Hu MX, Chu HY and Zhang HW: miR-29a up-regulation in AR42J cells contributes to apoptosis via targeting TNFRSF1A gene. World J Gastroenterol 22: 4881-4890, 2016.
12. Zhang Y, Yan L and Han W: Elevated level of miR-551b-5p is associated with inflammation and disease progression in patients with severe acute pancreatitis. Ther Apher Dial 22: 649-655, 2018.
13. Xu XZ, Li XA, Luo Y, Liu JF, Wu HW and Huang G: MiR-9 promotes synovial sarcoma cell migration and invasion by directly targeting CDH1. Int J Biochem Cell Biol 112: 61-71, 2019.
14. Wang J, Wang B, Ren H and Chen W: miR-9-5p inhibits pancreatic cancer cell proliferation, invasion and glutamine metabolism by targeting GOT1. Biochem Biophys Res Commun 509: 241-248, 2019.
15. Song G, Ma Z, Liu D, Qian D, Zhou J, Meng H, Zhou B and Song Z: Bone marrow-derived mesenchymal stem cells attenuate severe acute pancreatitis via regulation of microRNA-9 to inhibit necroptosis in rats. Life Sci 223: 9-21, 2019.
16. Qian D, Wei G, Xu C, He Z, Hua J, Li J, Hu Q, Lin S, Gong J, Meng H, *et al*: Bone marrow-derived mesenchymal stem cells (BMSCs) repair acute necrotized pancreatitis by secreting microRNA-9 to target the NF-κB1/p50 gene in rats. Sci Rep 7: 581, 2017.
17. Nandy D and Mukhopadhyay D: Growth factor mediated signaling in pancreatic pathogenesis. Cancers (Basel) 3: 841-871, 2011.
18. Ndlovu R, Deng LC, Wu J, Li XK and Zhang JS: Fibroblast growth factor 10 in pancreas development and pancreatic cancer. Front Genet 9: 482, 2018.
19. Jakkampudi A, Jangala R, Reddy BR, Mitnala S, Nageshwar Reddy D and Talukdar R: NF-κB in acute pancreatitis: Mechanisms and therapeutic potential. Pancreatology 16: 477-488, 2016.
20. Liu W, Wang X, Zheng Y, Shang G, Huang J, Tao J and Chen L: Electroacupuncture inhibits inflammatory injury by targeting the miR-9-mediated NF-κB signaling pathway following ischemic stroke. Mol Med Rep 13: 1618-1626, 2016.
21. Gu R, Liu N, Luo S, Huang W, Zha Z and Yang J: MicroRNA-9 regulates the development of knee osteoarthritis through the NF-kappaB1 pathway in chondrocytes. Medicine (Baltimore) 95: e4315, 2016.
22. Li YH, Fu HL, Tian ML, Wang YQ, Chen W, Cai LL, Zhou XH and Yuan HB: Neuron-derived FGF10 ameliorates cerebral ischemia injury via inhibiting NF-κB-dependent neuroinflammation and activating PI3K/Akt survival signaling pathway in mice. Sci Rep 6: 19869, 2016.
23. Chen J, Wang Z, Zheng Z, Chen Y, Khor S, Shi K, He Z, Wang Q, Zhao Y, Zhang H, *et al*: Neuron and microglia/macrophage-derived FGF10 activate neuronal FGFR2/PI3K/Akt signaling and inhibit microglia/macrophages TLR4/NF-κB-dependent neuroinflammation to improve functional recovery after spinal cord injury. Cell Death Dis 8: e3090, 2017.
24. Livak KJ and Schmittgen TD: Analysis of relative gene expression data using real-time quantitative PCR and the 2(-Delta Delta C(T)) method. Methods 25: 402-408, 2001.
25. Wang Y, Wang G, Cui L, Liu R, Xiao H and Yin C: Angiotensin 1-7 ameliorates caerulein-induced inflammation in pancreatic acinar cells by downregulating Toll-like receptor 4/nuclear factor-κB expression. Mol Med Rep 17: 3511-3518, 2018.
26. Zhao D, Ge H, Ma B, Xue D, Zhang W, Li Z and Sun H: The interaction between ANXA2 and lncRNA Fendrr promotes cell apoptosis in caerulein-induced acute pancreatitis. J Cell Biochem 120: 8160-8168, 2019.
27. Jaworek J, Szklarczyk J, Kot M, Góralska M, Jaworek A, Bonior J, Leja-Szpak A, Nawrot-Porąbka K, Link-Lenczowski P, Ceranowicz P, *et al*: Chemerin alleviates acute pancreatitis in the rat thorough modulation of NF-κB signal. Pancreatology 19: 401-408, 2019.
28. Qian D, Song G, Ma Z, Wang G, Jin L, Hu M, Song Z and Wang X: MicroRNA-9 modified bone marrow-derived mesenchymal stem cells (BMSCs) repair severe acute pancreatitis (SAP) via inducing angiogenesis in rats. Stem Cell Res Ther 9: 282, 2018.
29. Lu P, Wang F, Wu J, Wang C, Yan J, Li ZL, Song JX and Wang JJ: Elevated serum miR-7, miR-9, miR-122, and miR-141 are noninvasive biomarkers of acute pancreatitis. Dis Markers 2017: 7293459, 2017.
30. Lesina M, Wörmann SM, Neuhöfer P, Song L and Algül H: Interleukin-6 in inflammatory and malignant diseases of the pancreas. Semin Immunol 26: 80-87, 2014.
31. Yi J and Gao ZF: MicroRNA-9-5p promotes angiogenesis but inhibits apoptosis and inflammation of high glucose-induced injury in human umbilical vascular endothelial cells by targeting CXCR4. Int J Biol Macromol 130: 1-9, 2019.
32. Yang Y, Huang Q, Luo C, Wen Y, Liu R, Sun H and Tang L: MicroRNAs in acute pancreatitis: From pathogenesis to novel diagnosis and therapy. J Cell Physiol 235: 1948-1961, 2020.
33. Warzecha Z, Dembinski A, Ceranowicz P, Dembinski M, Kownacki P, Konturek SJ, Tomaszewska R, Stachura J, Hładki W and Pawlik WW: Immunohistochemical expression of FGF-2, PDGF-A, VEGF and TGF beta RII in the pancreas in the course of ischemia/reperfusion-induced acute pancreatitis. J Physiol Pharmacol 55: 791-810, 2004.
34. Andoh A, Bamba S, Fujino S, Inatomi O, Zhang Z, Kim S, Takayanagi A, Shimizu N and Fujiyama Y: Fibroblast growth factor-2 stimulates interleukin-6 secretion in human pancreatic periacinar myofibroblasts. Pancreas 29: 278-283, 2004.
35. Ishiwata T, Naito Z, Lu YP, Kawahara K, Fujii T, Kawamoto Y, Teduka K and Sugisaki Y: Differential distribution of fibroblast growth factor (FGF)-7 and FGF-10 in L-arginine-induced acute pancreatitis. Exp Mol Pathol 73: 181-190, 2002.
36. Zhou P, Hua F, Wang X and Huang JL: Therapeutic potential of IKK-β inhibitors from natural phenolics for inflammation in cardiovascular diseases. Inflammopharmacology 28: 19-37, 2020.
37. Perkins ND: The diverse and complex roles of NF-κB subunits in cancer. Nat Rev Cancer 12: 121-132, 2012.

38. Hoesel B and Schmid JA: The complexity of NF-κB signaling in inflammation and cancer. Mol Cancer 12: 86, 2013.
39. Liu Z, Liu J, Zhao K, Shi Q, Zuo T, Wang G and Wang W: Role of daphnetin in rat severe acute pancreatitis through the regulation of TLR4/NF-[Formula: see text]B signaling pathway activation. Am J Chin Med 44: 149-163, 2016.
40. Zhao S, Yang J, Liu T, Zeng J, Mi L and Xiang K: Dexamethasone inhibits NF-κBp65 and HMGB1 expression in the pancreas of rats with severe acute pancreatitis. Mol Med Rep 18: 5345-5352, 2018.
41. Jo IJ, Bae GS, Choi SB, Kim DG, Shin JY, Seo SH, Choi MO, Kim TH, Song HJ and Park SJ: Fisetin attenuates cerulein-induced acute pancreatitis through down regulation of JNK and NF-κB signaling pathways. Eur J Pharmacol 737: 149-158, 2014.
42. Jiang CY and Wang W: Resistin aggravates the expression of proinflammatory cytokines in ceruleinstimulated AR42J pancreatic acinar cells. Mol Med Rep 15: 502-506, 2017.
43. Zhu M, Xu Y, Zhang W, Gu T and Wang D: Inhibition of PAK1 alleviates cerulein-induced acute pancreatitis via p38 and NF-κB pathways. Biosci Rep 39: BSR20182221, 2019.